ISSN: 2321-2152

IJMECE

International Journal of modern electronics and communication engineering

E-Mail
editor.ijmece@gmail.com
editor@ijmece.com

www.ijmece.com

ISSN2321-2152
www.ijmece .com
volume 12 issue 2,2024

Fuzzy-Logic Controlled EV charging station with integrated distributed energy sources for grid connectivity

Shaik Imran[1], M. Suresh Kumar[2]
[1]PG Student, Department of EPS, PVKK Institute of Technology, Anantapur
[2]Asssitant Professor, Department of EEE, PVKK Institute of Technology, Anantapur

ABSTRACT:

This paper introduces a cutting-edge Electric Vehicle (EV) charging station designed to seamlessly integrate with the grid while utilizing Distributed Energy Resources (DERs). Employing a Fuzzy Logic Controller, the system dynamically manages energy flow, optimizing charging processes and grid interactions. The integration of DERs, including solar panels and energy storage, enhances the station's self-sufficiency and resilience. The Fuzzy Logic Controller intelligently adapts to varying conditions, considering factors such as grid demand, renewable energy availability, and charging requirements. This adaptive control ensures efficient energy utilization, minimizes environmental impact, and supports grid stability. The charging station serves as a sustainable and intelligent node in the evolving energy landscape, promoting widespread EV adoption while contributing to a resilient and eco-friendly energy infrastructure. The proposed solution aligns with the growing emphasis on smart grid technologies and decentralized energy sources, showcasing a practical implementation of Fuzzy Logic for optimized EV charging within a distributed energy ecosystem.

KEY WORDS:

Solar generation, Inverter, PI controllers, Power Quality, MPPT, Bi-directional Dc-Dc converter, Adaptive comb-filter, distribution network, EV charging, fuel cell stack, grid connected mode, islanded mode, power quality, seamless power transfer, Fuzzy Logic Controller.

INTRODUCTION:

In the existing system, the smart grid integration of EV charging stations to reduce harmonic distortion losses and improve power quality is presented. Prevalent control techniques, such as the second-order generalized integrator (SOGI), the least mean fourth (LMF) control mechanism, and a robust control technique, are utilized here for charging EVs with seamless connection to the grid. Disadvantages of the existing system included: Complexity, Excessive charging of the storage battery,

ISSN2321-2152
www.ijmece .com
volume12 issue 2,2024

Maintenance, Inoperative PV panel with disconnection of grid.

The proposed system utilizes an adaptive comb-filter for power quality improvement during grid interconnection and EV charging. Seamless transitions between grid-connected and disconnected modes of operation are achieved in the common DC bus EV charging system. The use of hybrid distributed energy sources, such as a solar PV array, battery, and fuel cell stack. So, in order to reduce these issues we are using Fuzzy Logic Controller. It enhances system performance by maintaining good power quality.

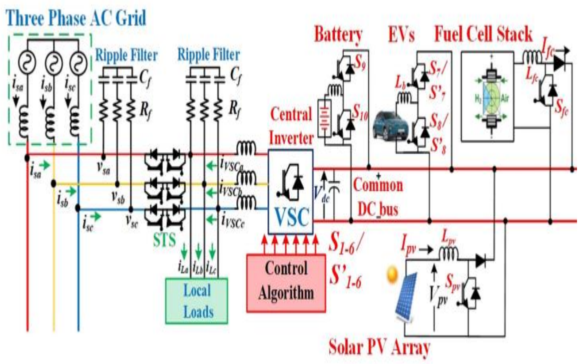

Fig: Block Diagram of EVs charging system configuration with hybrid renewable energy sources.

Advantages of the proposed system includes: Decarbonization, Bidirectional charging improved power quality,

Applications of the proposed system includes: Emergency Backup power, Hybrid microgrid, energy independence, Electric vehicle charging, Electric vehicle charging stations.

EXISTING SYSTEM:

In the existing system, the smart grid integration of EV charging stations to reduce harmonic distortion losses and improve power quality is presented. Prevalent control techniques, such as the second-order generalized integrator (SOGI), the least mean fourth (LMF) control mechanism, and a robust control technique, are utilized here for charging EVs with seamless connection to the grid. Disadvantages are Complexity, excessive charging of the storage battery, Maintenance, Inoperative PV panel with disconnection of grid.

PROPOSED SYSTEM:

In the proposed system, the source of power to the electrical vehicles to be solar PV array, Fuel cell, Battery. The fuel cell has high specific energy and ultra flywheel which has high specific power its possible to increase the driving range get a performance similar to ICEV.

Adaptive comb filter in hybrid electric vehicles are used for noise cancellation and filtering out unwanted frequencies from signals, especially in power electronics systems. They help improve the performance and efficiency of the vehicles electric powertrain by reducing electromagnetic interference and enhancing

ISSN2321-2152
IJMECE
www.ijmece .com
volume 12 issue 2,2024

the quality of electrical signals. This can result in the smoother operation and better overall performance of the hybrid system.

During the grid connected mode of operation, the Static Transfer Switch (STS switch) are to be placed in working so that the power source to the Electric vehicle has to be done in the presence of the grid connection mode of operation. By using the Fuzzy logic controller we can enhance the efficiency of the system due to its advanced controlling techniques when compared to the Proportional- Integrator controller techniques. Hence overall the system performance to be enhanced and the Power Quality to be increased by experimentally in the sense of decreasing Total Harmonic Distortion (THD).

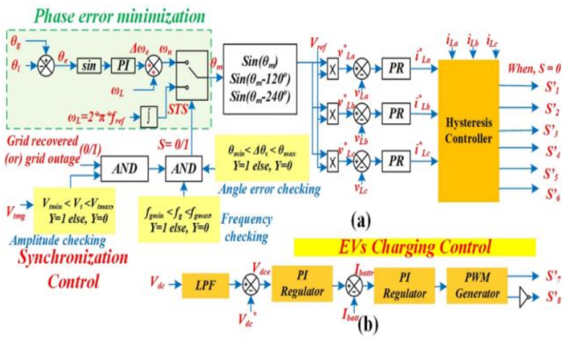

Fig: Control of operation during grid presence.

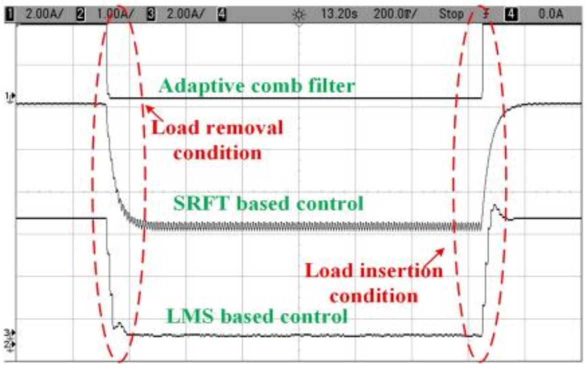

Fig: Comparative performance with respect to the weight convergence

Grid-Tied Mode of Operation for Common DC Bus EVs Charging System. The grid line voltages (v_{sab}, v_{sbc}) are utilized to estimate the grid phase voltages as

$$v_{sa} = \frac{v_{sbc}}{3} + \frac{2v_{sab}}{3}, v_{sb} = \frac{v_{sbc}}{3} - \frac{v_{sab}}{3}, \quad v_{sc} = -\frac{2v_{sbc}}{3} - \frac{v_{sab}}{3} \tag{1}$$

Thus, by using obtained grid phase voltages (v_{sa}, v_{sb}, v_{sc}), the terminal voltage (Vt) is evaluated as

$$V_t = \sqrt{2(v_{sa}^2 + v_{sb}^2 + v_{sc}^2)/3} \tag{2}$$

The v_{sa}, v_{sb}, v_{sc} and V_t are utilized to obtain u_{pa}, u_{pb}, u_{pc} and u_{qa}, u_{qb}, u_{qc} as,

$$u_{pa} = v_{sa}/V_t, u_{pb} = v_{sb}/V_t, u_{pc} = v_{sc}/V_t$$

$$u_{qa} = \frac{-u_{pb}}{\sqrt{3}} + \frac{u_{pc}}{\sqrt{3}}, u_{qb} = \frac{3u_{pa}}{2\sqrt{3}} + \frac{u_{pb}}{2\sqrt{3}} - \frac{u_{pc}}{2\sqrt{3}}, u_{qc} = \frac{-3u_{pa}}{2\sqrt{3}} + \frac{u_{pb}}{2\sqrt{3}} - \frac{u_{pc}}{2\sqrt{3}}$$

Moreover, the charging of EVs during the grid connected mode of operation, enables obtaining requisite energy from the grid for charging or returning the surplus renewable generation to the grid for storage purposes at an improved power quality. Thus, the charging of EVs is obtained using a cascaded

PI constant current/ constant voltage controller for generating the switching pulses (S7 and S8) of the bidirectional converter as presented in Fig. 2(c). The sensed (Vev) and the reference voltages (V ∗ ev) of EVs are utilized to obtain the voltage error (Veve) as

$$V_{eve} = V^*_{ev} - V_{ev} \quad ($$

The output voltage error (Veve) obtained is utilized to obtain the reference current (I∗ ev) of the EVs as follows:

$$I^*_{ev}(m) = I^*_{ev}(m-1) + K_{pev}\{V_{eve}(m)\} + K_{iev}\{V_{eve}(m) - V_{eve}(m-1)\} \quad (6)$$

Furthermore, the current error I_{eve} is obtained as follows

$$I_{eve} = I^*_{ev} - I_{ev} \quad (7)$$

The current error (Ieve) obtained fed to a PI controller for generation of duty cycle for PWM switching pulses S7 and S8

$$D_{eve}(m) = D_{eve}(m-1) + K_{peve}\{I_{eve}(m)\} + K_{ieve}\{I_{eve}(m) - I_{eve}(m-1)\} \quad (8)$$

Moreover, in order to enable the charging/discharging of the battery, the DC link voltage error is evaluated as,

$$V_{dce} = V^*_{dc} - V_{dc} \quad (9)$$

The estimated DC link voltage error obtained is utilized to obtain the reference battery current (I∗ batt) as follows,

$$I^*_{batt}(m) = I^*_{batt}(m-1) + K_{pdc}\{V_{dce}(m)\} + K_{idc}\{V_{dce}(m) - V_{dce}(m-1)\} \quad (10)$$

The I∗ batt is compared with the sensed battery current (I_{batt}) as

$$I_{battr} = I^*_{batt} - I_{batt} \quad (11)$$

The obtained current error is given to the PI current controller to estimate the duty ratio for the bidirectional converter switching pulses S9-S10 in Fig as,

$$D(m) = D(m-1) + K_{pbatt}\{I_{battr}(m)\} + K_{ibatt}\{I_{battr}(m) - I_{battr}(m-1)\} \quad (12)$$

The advantages of utilizing a comb-filter, lie in its simple structure as its implementation utilizes only delays, adders and subtractions. Therefore, the adaptive comb-filter is utilized for obtaining the fundamental load current ifLa. The transfer function for estimating the fundamental of load current with the utilization of a comb-filter is given as,

$$\frac{i_{Lfa}}{i_{La}} = \frac{1}{M^2}\frac{\alpha(1-z^{-M})\delta(1-z^{M})}{(1-z^{-1})(1-z)} \quad (13)$$

Where, M = fs/fM, fs is the sampling frequency, fM is the fundamental of the periodic frequency and α, δ are the gains of the filter. Therefore, in order to set the gains of the filter with the existing cut-off frequency (ωc0) and the desired cut-off frequency (ωcα), the parameter α is obtained as [17],

$$\alpha = \left[\frac{\tan x}{\sin\omega_{c\alpha} + \tan x\cos\omega_{c\alpha}}\right], x = \frac{M\omega_{c0} - \omega_{c\alpha}}{2} \quad (14)$$

Thus, on further simplification, the transfer function obtained for the adaptive comb filter is given as follows,

$$\frac{i_{Lfa}}{i_{La}} = \frac{\alpha z^{-1}(\delta_1+\gamma_1) - \left(\frac{\alpha(1-\gamma_1)}{z^{-1}}\right)\delta_1 - \left(\frac{\alpha(1-\delta_1)}{z^{-1}}\right)\gamma_1}{\delta_1\gamma_1} \quad (15)$$

Therefore, the fundamental component of the load current i_{Lfa} obtained is free from harmonics and sinusoidal in nature. The i_{Lfa} acquired is passed through zero crossing detector (ZCD), which is also provided with the quadrature phase unit templates (uqa, uqb, uqc). Consequently, after passing through the absolute block, load active power component (I_{fpa}) is obtained. Similarly, I_{fpb} and Ifpc are determined and the average of load currents fundamental (I_{fpa}, I_{fpb}, I_{fpc}) component is estimated as,

$$I_{pLavg} = (I_{fpb} + I_{fpc} + I_{fpa})/3 \quad (16)$$

Moreover, an INC based MPPT mechanism for maximum power extraction is utilized as presented In Fig. 2(d). The PV feed-forward w_{pv} is calculated as

$$w_{pv} = (2P_{pv})/(3V_t) \quad (17)$$

Furthermore, the control of the fuel cell is utilized through the efficient switching of (Sfc), which is obtained by PWM generator. The maximum power of the fuel cell is extracted through a MPPT technique as shown in Fig. 2(b) and the feed-forward term of the fuel cell, in order to improve the convergence rate is

$$w_{fc} = (2P_{fc})/(3V_t)$$

Moreover, the contribution of the battery and EVs is given as,

$$w_{batt} = (2P_{batt})/(3V_t), w_{ev} = (2P_{ev})/(3V_t) \quad (19)$$

In order to obtain the grid active power component, the load active power component, PV feed forward term, contribution of battery and fuel cell are utilized as,

$$I_{pnet} = I_{pLavg} - (w_{pv} + w_{fc} + w_{batt} + w_{ev}) \quad (20)$$

$$i^*_{sa} = u_{pa} \times I_{pnet}, i^*_{sb} = u_{pb} \times I_{pnet}, i^*_{sc} = u_{pc} \times I_{pnet} \quad (21)$$

The current errors as obtained below are passed to the hysteresis controller for the generation of switching pulses S1-6 during grid connected mode of operation,

$$i_{esa} = i^*_{sa} - i_{sa}, i_{esb} = i^*_{sb} - i_{sb}, i_{esc} = i^*_{sc} - i_{sc} \quad (22)$$

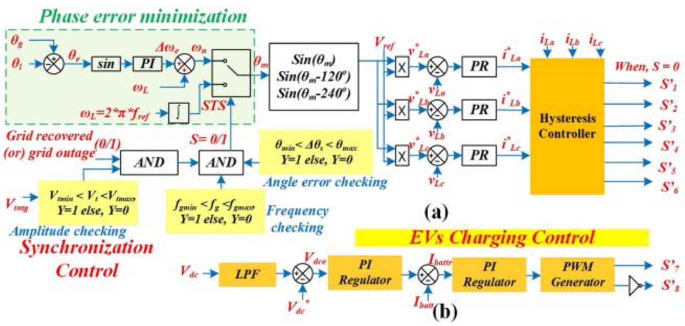

Fig: Control for operation during grid absence.

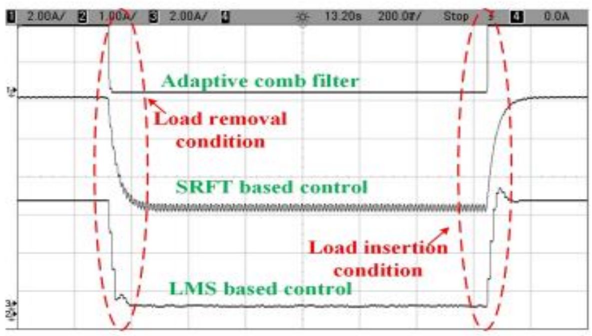

Fig: Comparative performance with respect to the weight convergence.

During the standalone mode as shown in Fig. 3(a), a voltage control is employed and the condition of grid unavailability is presented by STS signal equal to ‘0’. The reference load voltages ($v*_{La}$, $v*_{Lb}$, $v*_{Lc}$) are evaluated as follows

$$v^*_{La} = V_{ref} \times \sin\theta_m, v^*_{Lb} = V_{ref} \times \sin(\theta_m - 120°),$$
$$v^*_{Lc} = V_{ref} \times \sin(\theta_m - 240°) \qquad (23)$$

Where, V_{ref} is the amplitude of the load voltages, which is obtained from the three-phase load voltages and θ_m is the load voltage angle. The PR controller [18] is utilized for generating the reference load currents ($i*_{La1}$, $i*_{Lb1}$, $i*_{Lc1}$) by utilizing the voltage error obtained from sensed and reference load voltages as follows,

$$i^*_{La} = T_a(s) \times v_{Lae}(s)$$
$$= \left\{k_{pae} + \frac{(k_{iae}2\omega_c s)}{(s^2 + 2\omega_c s + \omega_r^2)}\right\} \times v_{Lae}(s) \qquad (24)$$
$$i^*_{Lb} = T_b(s) \times v_{Lbe}(s)$$
$$= \left\{k_{pbe} + \frac{(k_{ibe}2\omega_c s)}{(s^2 + 2\omega_c s + \omega_r^2)}\right\} \times v_{Lbe}(s) \qquad (25)$$
$$i^*_{Lc} = T_c(s) \times v_{Lce}(s) = \left\{k_{pce} + \frac{(k_{ice}2\omega_c s)}{(s^2 + 2\omega_c s + \omega_r^2)}\right\} \times v_{Lce} \qquad (26)$$

Consequently, by passing the current errors as obtained below through the hysteresis controller VSC pulses S’1-S’6 are obtained.

$$i_{eLa} = i^*_{La} - i_{La}, i_{eLb} = i^*_{Lb} - i_{Lb}, i_{eLc} = i^*_{Lc} - i_{Lc} \qquad (27)$$

The EV charging during standalone mode of operation is obtained through the control mechanism presented in Fig. 3(b). Here, the reference and sensed DC link voltages are used to obtain the error, which is further evaluated to obtain reference current of battery and through PWM switching the bidirectional pulses (S’ 7-S’ 8) are obtained

Simulation Results :

The synchronization control for common DC bus charging of EVs with distributed microgrid consisting of solar PV array, battery and fuel cell sources, is shown in Fig. 3(a). For connecting the islanded distribution generation system to the utility grid, the voltages of islanded distribution generation system and their phase angles are synchronized to the grid voltages and their phase angles. After the estimation of phase angles, a PI controller is used, for matching the grid voltages and PCC voltages phase angles. Thus, the phase error between the grid and load voltage angles is estimated as,

$$\theta_e = \theta_g - \theta_L \qquad (28)$$

The phase error obtained is given to the PI controller, for determining frequency error as,

$$\Delta\omega_e(n) = \Delta\omega_e(n-1) + k_{pe}\{\theta_e(n) - \theta_e(n-1)\} + k_{Ie}\theta_e(n) \qquad (29)$$

Where, $\Delta_{\omega e}$ represents the frequency change. Therefore, the control sends the modified frequency (ω_n) = ($\Delta\omega e$ + ω_L) in case if the grid is recovered. However, the fundamental frequency

of load (ω_L) is utilized during standalone mode of operation. In addition, with the multiplication of the amplitude of load voltage (V_{ref}) with the load voltage angle (θ_m) obtained from this frequency, is utilized for obtaining the three-phase reference load voltages.

ISSN2321-2152
www.ijmece .com
volume 12 issue 2,2024

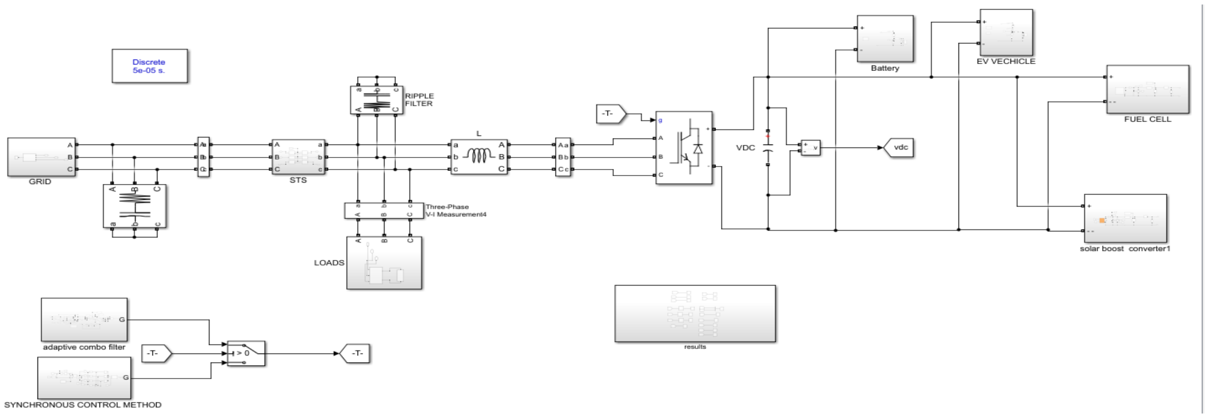

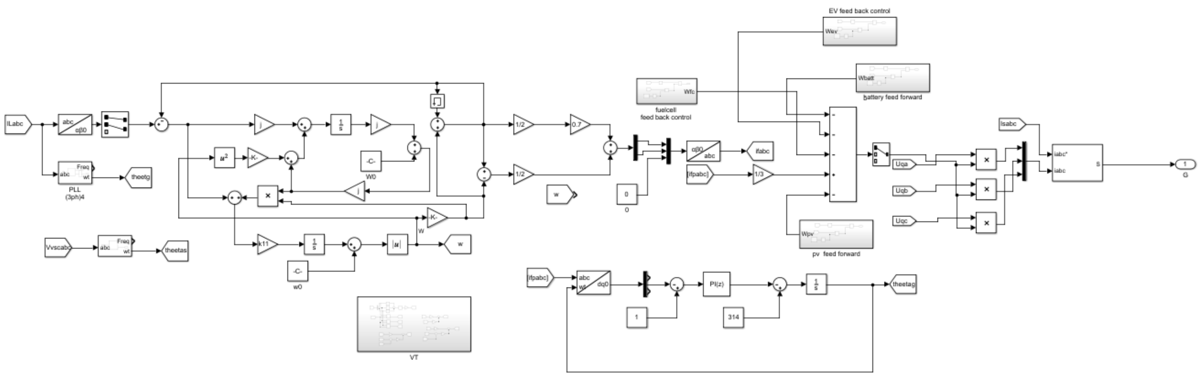

Adaptive Comb filter

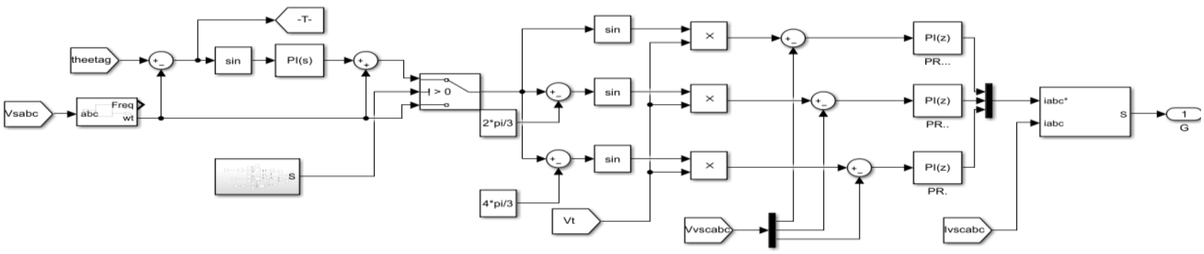

Synchronization model

Mode change from grid-tied to standalone operation for common DC bus EVs charging system

ISSN2321-2152

IJMECE

www.ijmece .com
volume 12 issue 2,2024

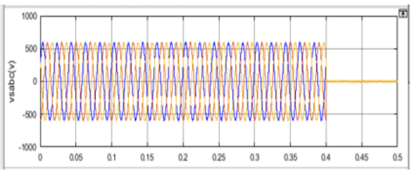

Vsabc(v)

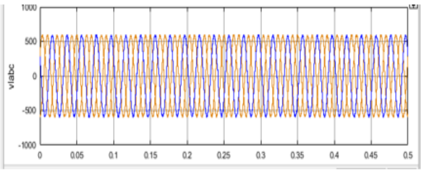

Vlabc (v)

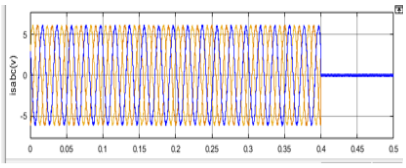

ISabc

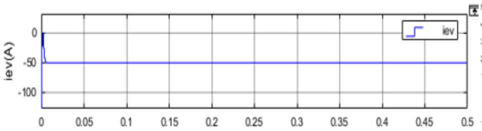

Iev(A)

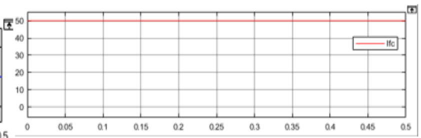

Ifc

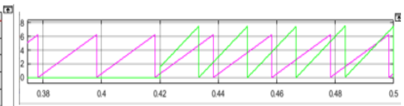

Theethag&thetas

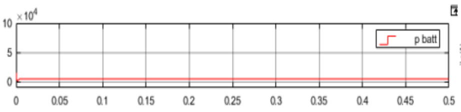

P batt(w)

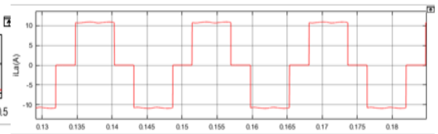

Ila(A)

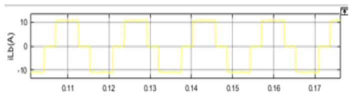

iLb(A)

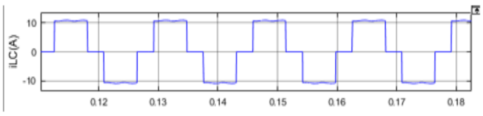

iLC(A)

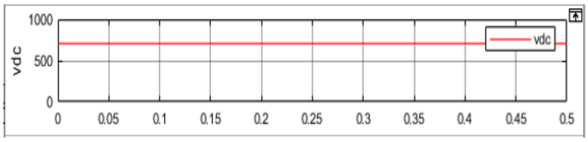

Vdc

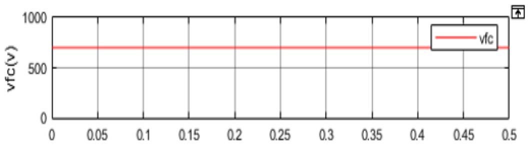

Vfc(v)

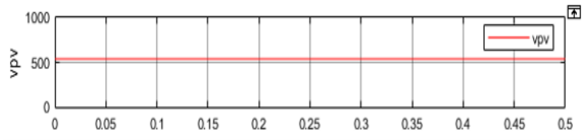

Vpv

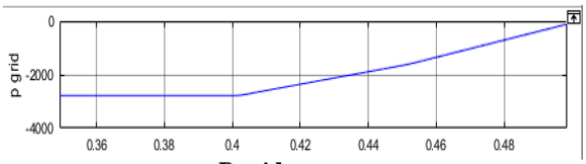

P grid

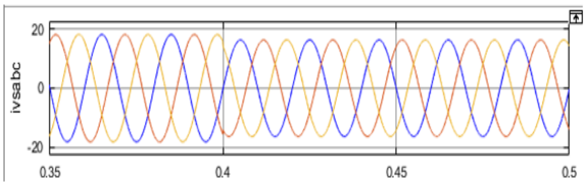

Ivsabc

ISSN2321-2152

www.ijmece .com
volume 12 issue 2,2024

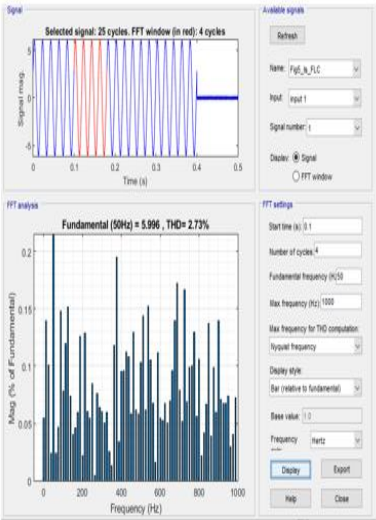

THD of Grid Current

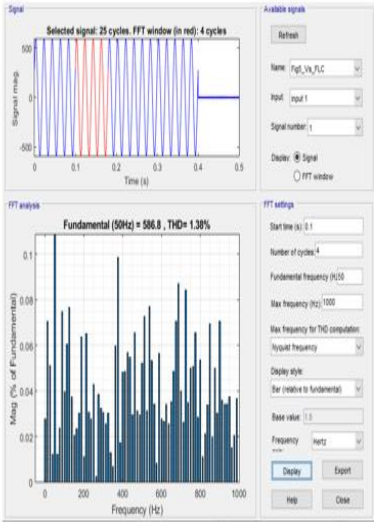

THD of Grid Voltage

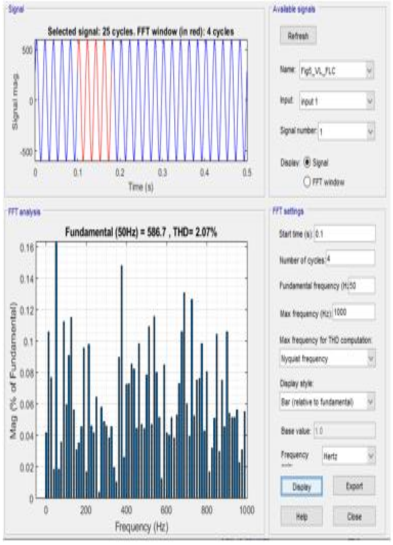

THD of Load Voltage

Mode change from grid-tied to standalone operation for common DC bus EVs charging system

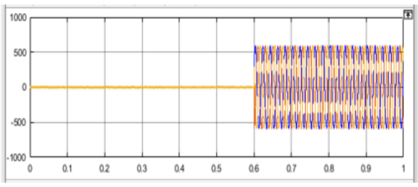

Vsabc

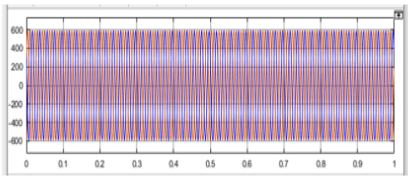

Vlabc

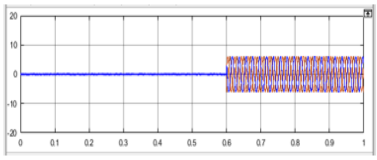

Isabc

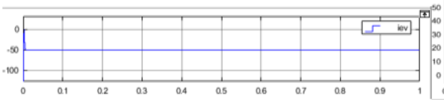

Iev

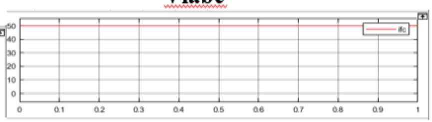

Ifc

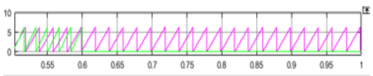

Theethag&the ethas

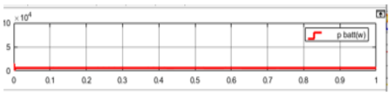

P batt

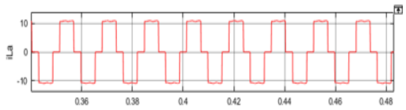

ila

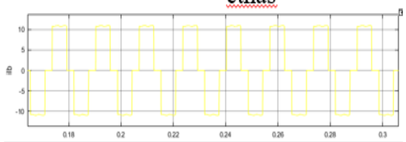

Ilb

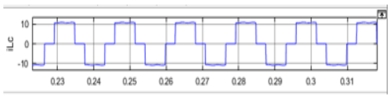

iLc

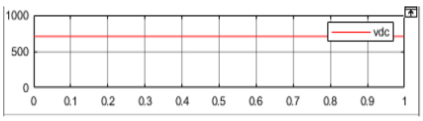

Vdc

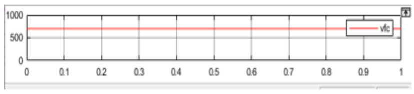

Vfc

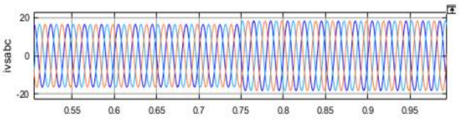

Ivsabc

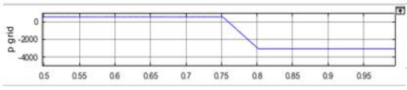

P grid

Vpv

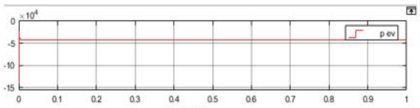

P EV

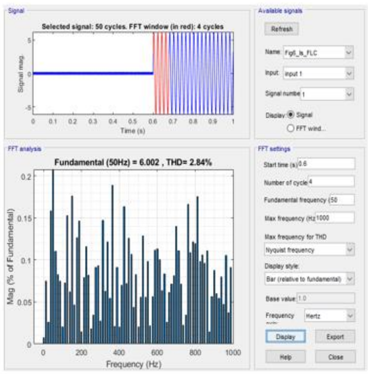

THD of Grid Current

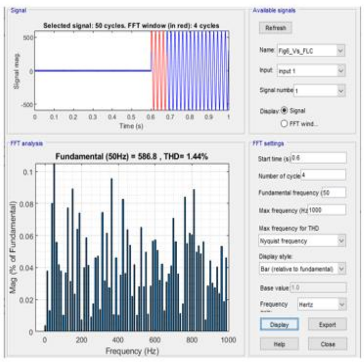

THD of Grid Voltage

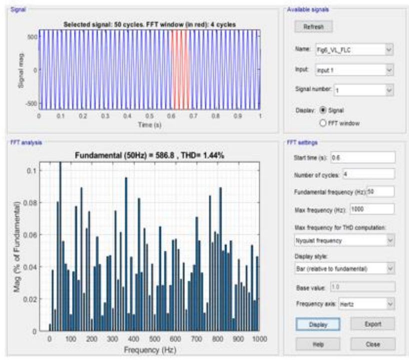

THD of Load Voltage

Mode change from standalone grid-tied to operation for common DC bus EVs charging system

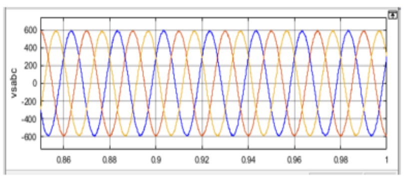

Vsabc

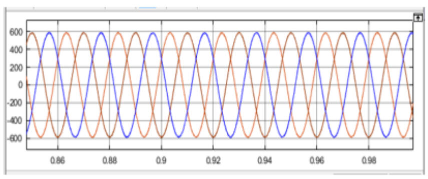

Vlabc

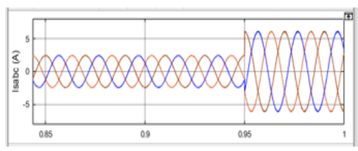

Isabc

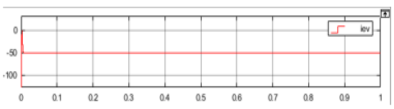

I ev

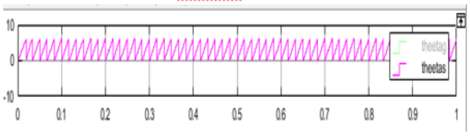

Theetha g&thetas

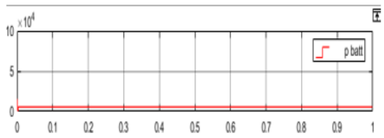

P batt

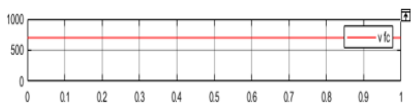

V fc

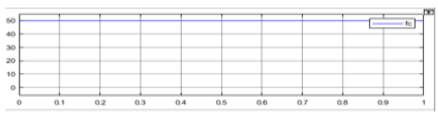

Fuel cell current

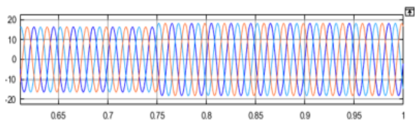

Ivsabc

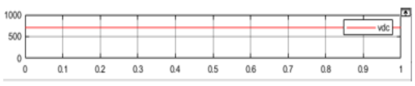

Vdc

Vpv

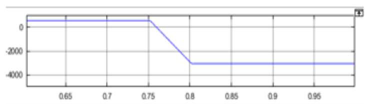

Ppv

ISSN2321-2152

www.ijmece .com
volume 12 issue 2,2024

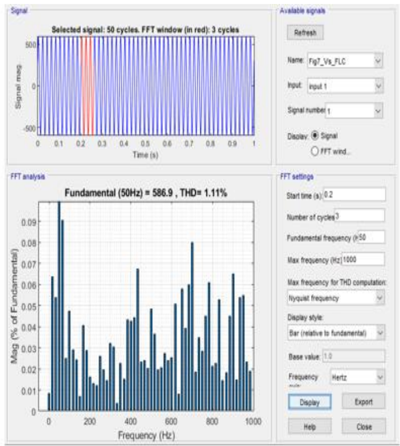

THD of Grid Voltage

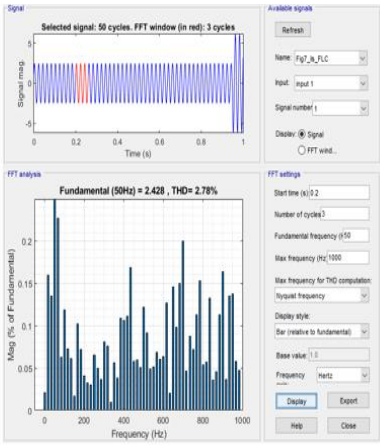

THD of Grid Current

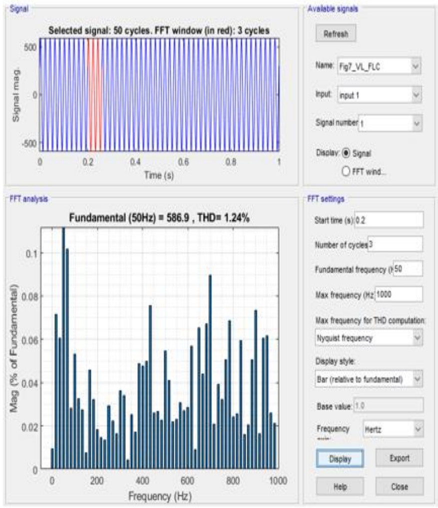

THD of Load Voltage

Performance of common DC bus EVs charging system during load unbalancing condition

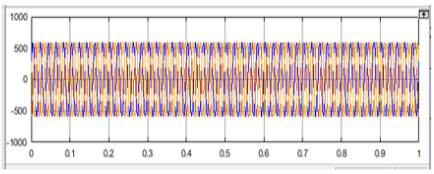

Vsabc

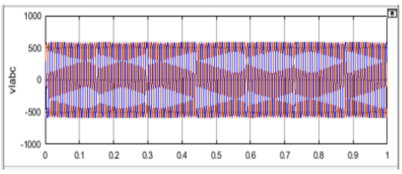

Vlabc

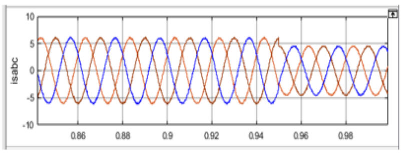

Isabc

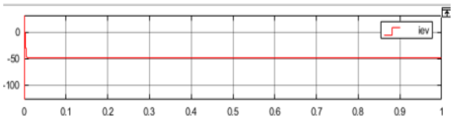

I ev

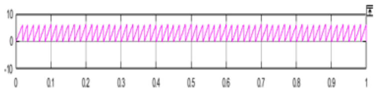

Theetag &theetas

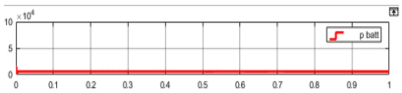

P batt

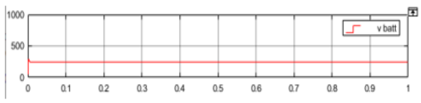

V batt

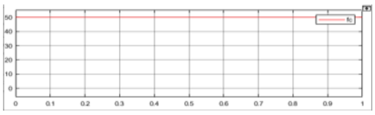

Fc

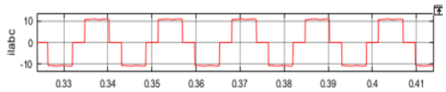

Ilabc

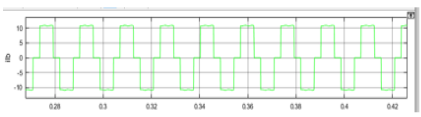

Ilb

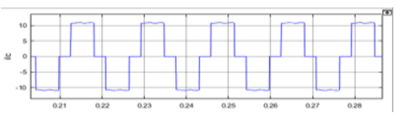

Ilc

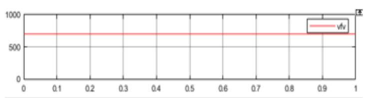

Vfv

ISSN2321-2152

www.ijmece .com
volume 12 issue 2,2024

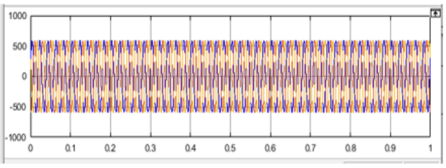

Vsabc

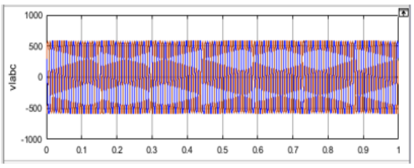

Vlabc

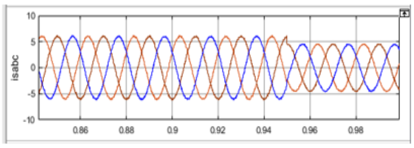

Isabc

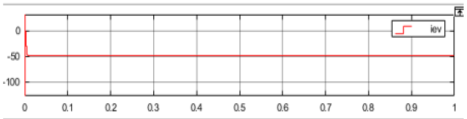

I ev

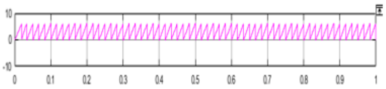

Theetag &theetas

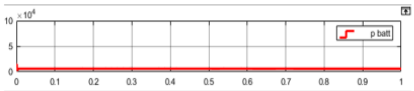

P batt

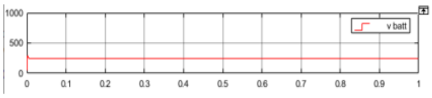

V batt

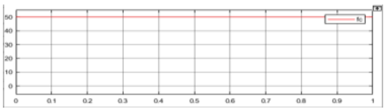

Fc

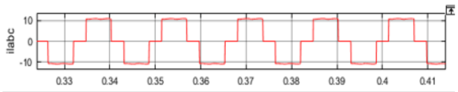

Ilabc

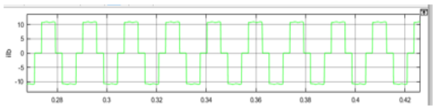

Ilb

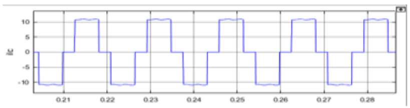

Ilc

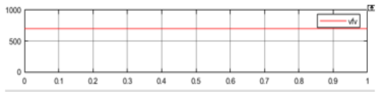

Vfv

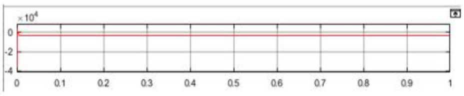

Pev

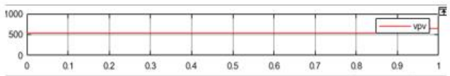

Vpv

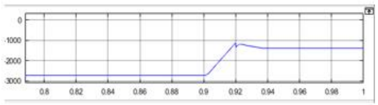

Ppv

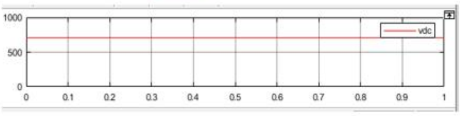

Vdc

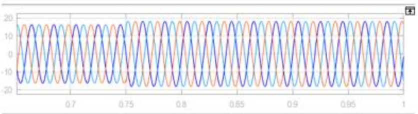

Ivsabc

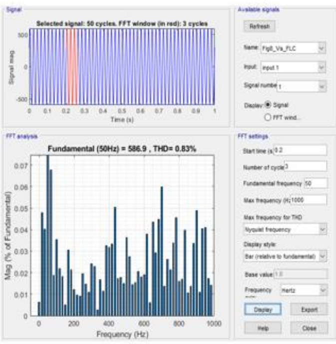

THD of Grid Voltage

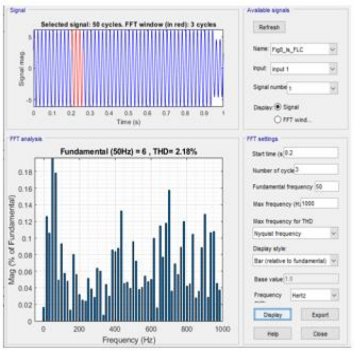

THD of Grid Current

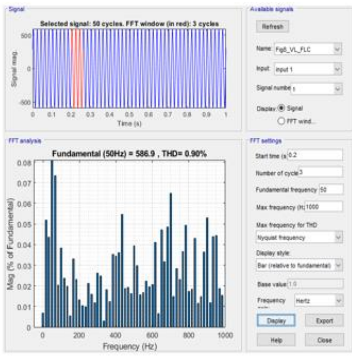

THD of Load Voltage

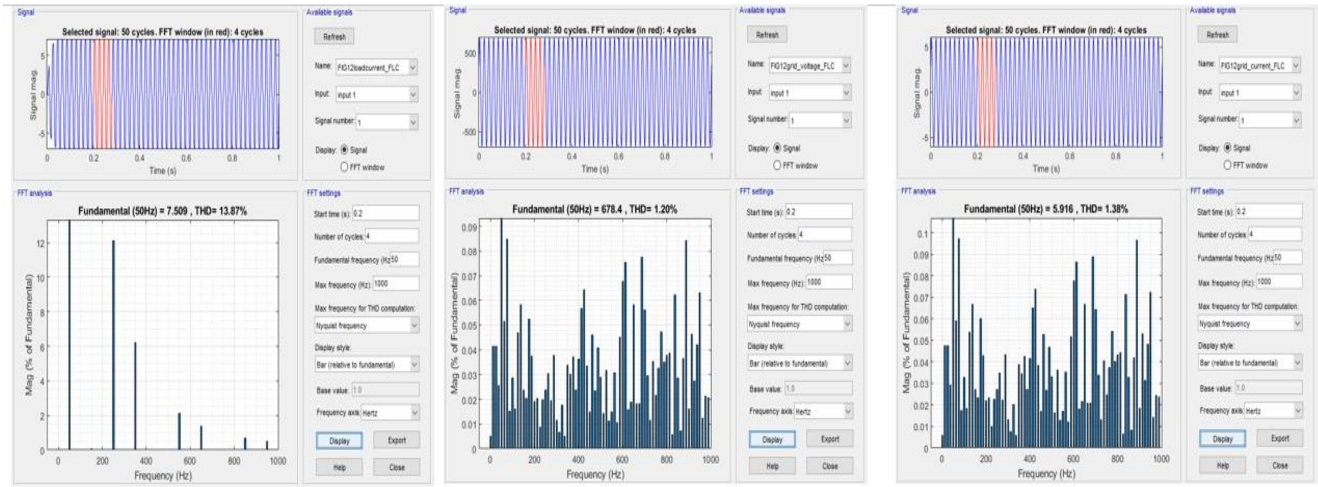

Load current   Grid voltage   Grid current

Harmonic analysis of grid-tied common DC bus EVs charging system.

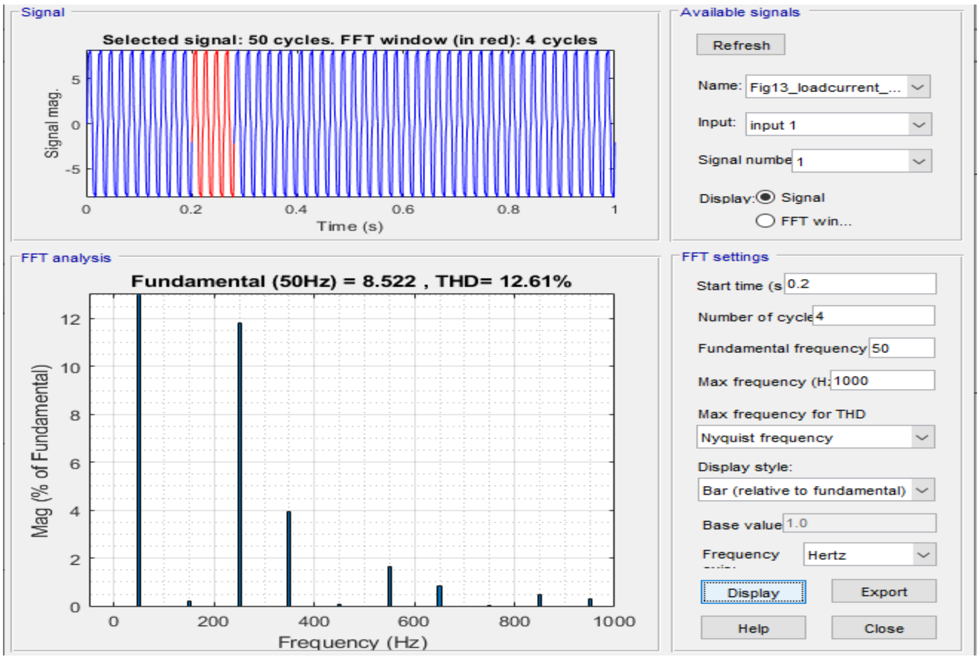

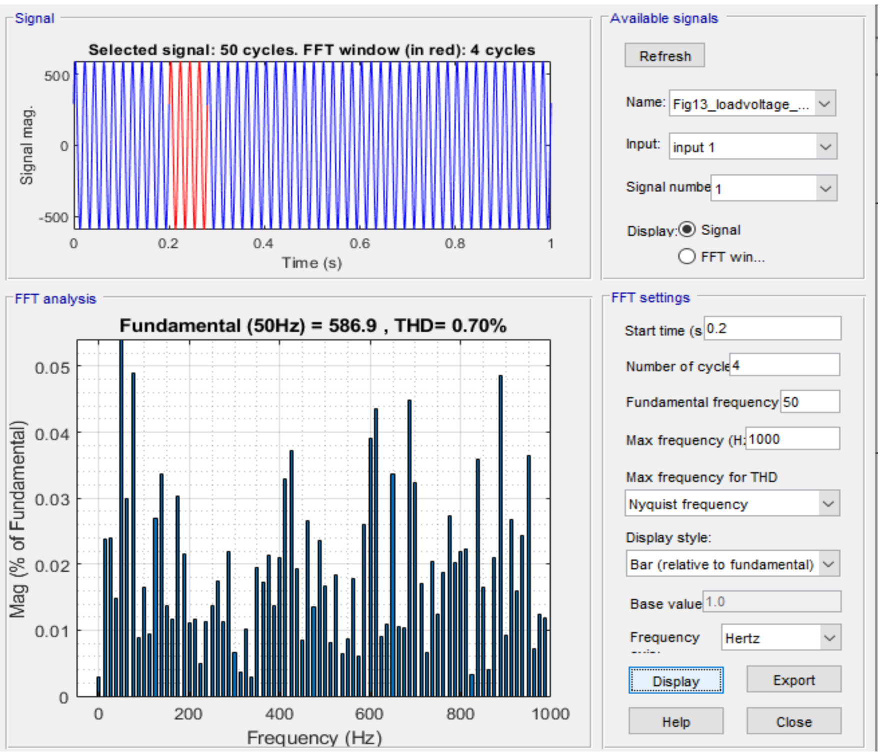

CONCLUSION:

The Fuzzy Logic-Controlled Electric Vehicle (EV) Charging Station with Integrated Distributed Energy Resources (DERs) for Grid Connectivity project presents an innovative and sustainable solution for the evolving energy landscape. By integrating DERs such as solar panels and energy storage with an EV charging station, the system demonstrates enhanced efficiency, reduced grid dependency, and increased utilization of renewable energy sources. The implementation of Fuzzy Logic control adds intelligence to the system, optimizing energy flow, and managing charging schedules based on dynamic conditions. This holistic approach not only promotes eco-friendly transportation but also contributes to grid stability and resilience. The project's adaptability to varying grid scenarios makes it a promising model for the future of smart and sustainable urban energy ecosystems, fostering the integration of electric mobility with renewable energy sources while ensuring efficient and reliable grid connectivity.

REFERENCES:

[1] C. Gonçalves, P. Pinson, and R. J. Bessa, "Towards data markets in renewable energy forecasting," IEEE Trans. Sustain. Energy, vol. 12, no. 1, pp. 533–542, Jan. 2021.

[2] X. Yang, Y. Zhang, F. Zhang, C. Xu, and B. Yi, "Enhancing utilization of PV energy in building microgrids via autonomous demand response," IEEE Access, vol. 9, pp. 23554–23564, 2021.

[3] R.-J. Wai and W.-H. Wang, "Grid-connected photovoltaic generation system," IEEE Trans. Circuits Syst., vol. 55, no. 3, pp. 953–964, Apr. 2008.
[4] S. Jain, J. Jiang, X. Huang, and S. Stevandic, "Modelling of fuel-cell-based power supply system for grid interface," in Proc. IEEE Joint Int. Conf. Power Syst. Technol. Power India Conf., 2008, pp. 1–8.
[5] F. Ahmad, M. S. Alam, S. M. Shariff, and M. Krishnamurthy, "A cost efficient approach to EV charging station integrated community microgrid: A case study of Indian power market," IEEE Trans. Transp. Electrify., vol. 5, no. 1, pp. 200–214, Mar. 2019.
[6] M. Patterson, N. F. Macia, and A. M. Kannan, "Hybrid microgrid model based on solar photovoltaic battery fuel cell system for intermittent load applications, " IEEE Trans. Energy Conv., vol. 30, no. 1, pp. 359–366, Mar. 2015.
[7] M. S. Islam, N. Mithulananthan, and K. Y. Lee, "Suitability of PV and battery storage in EV charging at business premises," IEEE Trans. Power Syst., vol. 33, no. 4, pp. 4382–4396, Jul. 2018.